Available online at www.sciencedirect.com
ScienceDirect
Tetrahedron
Tetrahedron 62 (2006) 10223–10236

1,3,4-Oxadiazole formation as traceless release in solid phase organic synthesis

Sara Cesarini, Nicoletta Colombo, Maurizio Pulici, Eduard R. Felder and Wolfgang K.-D. Brill*

Department of Chemistry, Nerviano Medical Science, Viale Pasteur 10, 20014 Nerviano (Mi), Italy

Received 10 February 2006; revised 18 July 2006; accepted 3 August 2006
Available online 1 September 2006

Abstract—Oxadiazoles were generated upon a dehydrative cyclization reaction with 2-acyl hydrazides bound to the polymeric support via one of their N atoms using TFAA as a dehydration agent.

1. Introduction

Oxadiazoles are important structural components in many pharmaceuticals and agrochemicals[1] due to their topology and electronic properties.[2] The most common synthesis of 1,3,4-oxadiazoles is the dehydration of 2-acyl hydrazides.[3]

Recent synthesis methodologies making use of solid-support-bound reagents[4] may be highly useful to adapt oxadiazole formation to parallel chemistry. Two reports on the synthesis of oxadiazoles on solid supports have addressed this subject.[5] Herein we report the development of a method producing libraries of oxadiazoles in an array format with minimal manipulations and independent of the solubility of starting materials or intermediates.

By analogy to our solid-phase-mediated synthesis of oxazoles,[6] we investigated the possibility of synthesizing oxadiazoles from 2-acyl hydrazides covalently attached to a solid phase via a nitrogen atom, *directly* involved in the oxadiazole formation. Such a process would require a linker between the oxadiazole and the polymeric support, which could be cleaved concomitantly with the dehydrative cyclization, merely leaving a lone electron pair on the product as a 'trace'. To our knowledge, oxadiazole formations involving *N*1-alkylated 2-acyl hydrazides have not yet been reported.

2. Results and discussion

The choice of the linker is essential for our proposed process (Scheme 1). We intended to use an acid labile linker, which would readily eliminate a polymer-bound cation upon cyclization of a support-bound 2-acyl hydrazide. Among the commonly used linkers, which may provide such a stabilized cation, we considered trityl (**VI**), MAMP (**VII**), and *o*-methoxybenzyl[7] (**VIII**). Preliminary attempts to synthesize 2-acyl hydrazides on trityl and MAMP resins had failed owing to steric constraints imposed by the linker. The rigidity of the 2-acyl hydrazides may be another factor, impeding access of reagents and solvents, thus complicating oxadiazole formation. Therefore, we focused on an *o*-methoxybenzyl linker attached to the polystyrene resin via a flexible 4-butyryloxy spacer (**VIII**).

Firstly, our process involved the attachment of the 2-acyl hydrazides (**2a**–**e**) onto a polystyrene support via a flexible 4(4-formyl-3-methoxyphenoxy)butyryl linker **1**. Then, the support-bound acyl hydrazones (**3a**–**e**) were reduced to hydrazides (**4a**–**e**) using commercial borane–pyridine complex.[8] The latter reagent gave reproducibly clean, quantitative reductions without any precipitation. Subsequent acylation of hydrazides **4a**–**e** afforded 2-acyl hydrazides **6a**–**q**. Since monitoring these intermediates by cleavage with TFA gave low recovery and complex mixtures, the support-bound hydrazones **3a**–**e** and hydrazides **4a**–**e** were analyzed by IR and MAS ^{1}H NMR. The use of DMF-d_7 was essential for the MAS ^{1}H NMR analysis, since it assured sufficient swelling of the resin, and narrow NMR signals (including NH) facilitating spectral interpretation. Mono-acylation was required in order to avoid the formation of symmetrically substituted oxadiazoles, bearing only R^2 groups. Where carboxylic acids R^2–CO_2H were utilized as precursors, mono-acylations were performed with isopropoxy carbonyl-based mixed anhydrides[9] or symmetrical anhydrides, readily synthesized from carboxylic acids and ethoxy acetylene.[10] Alternatively, when acylchlorides were utilized, preferably they were converted to pentafluorophenyl esters, producing

Keywords: Cyclative release; Traceless linker; Dehydration; TFAA; Transacylation.
* Corresponding author. Tel.: +39 033 158 1437; fax: +39 033 158 1347; e-mail: wolfgang.brill@nervianoms.com

0040–4020/$ - see front matter © 2006 Elsevier Ltd. All rights reserved.
doi:10.1016/j.tet.2006.08.016

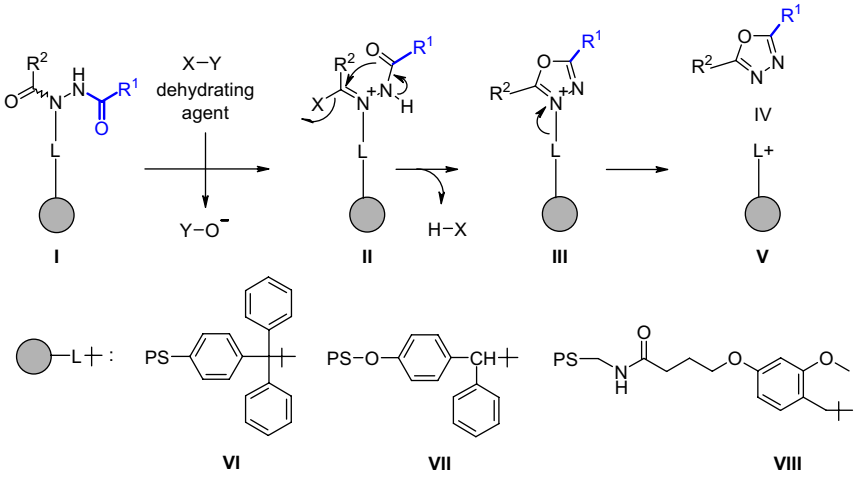

Scheme 1. Proposed oxadiazole formation on solid phase via cyclative release. PS: polystyrene; L: linker.

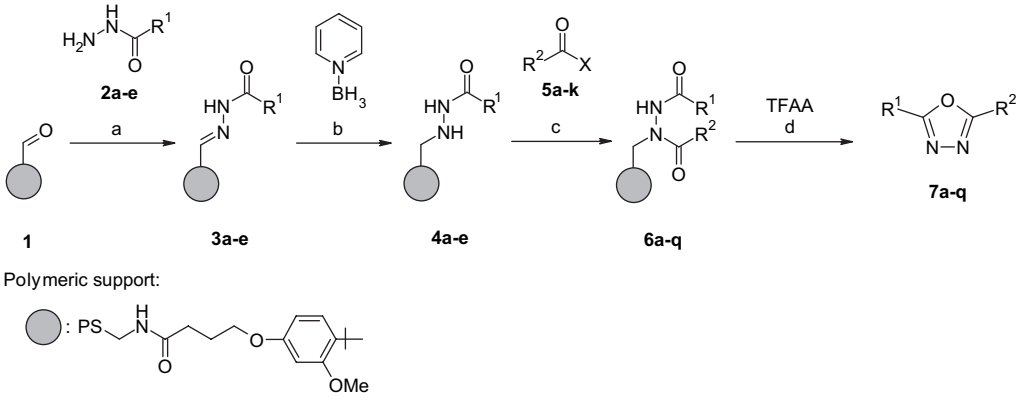

Scheme 2. Reagents and conditions: (a) 1.5 equiv **2a**–**e**, 1 equiv HOAc, CH_2Cl_2, 24 h, rt; (b) CH_2Cl_2–HOAc–pyridine·BH_3 (85:10:5, v/v/v), 8 h, rt; (c) 11 equiv anhydrides or pentafluorophenyl esters, NMI, CH_2Cl_2, 2 days, rt; (d) (i) TFAA–CH_2Cl_2–TFA (20:75:5, v/v/v), 5 h, rt; (ii) evaporation; (iii) MeOH, DOWEX1-X2 (carbonate form), 3 h, rt.

only mono-acylation products.[11] Additionally, we observed that the base was also crucial for the acylations. DIPEA (Hünig's base), TMEDA (*N*,*N*,*N*′,*N*′-tetramethylethylenediamine) or NMM (*N*-methylmorpholine) gave multiple acylations with hydrazides bearing CH-acidic carbons. NMI (*N*-methyl imidazole) appeared to be the base of choice, being a powerful, yet not too basic acylation catalyst. Finally, dehydrative, cyclative release of the oxadiazoles **7a**–**q** from the polymeric support was performed using volatile TFAA–CH_2Cl_2–TFA (20:75:5, v/v/v) (Scheme 2).

The cyclizations were completed in less than 5 h. Prolonged or multiple TFAA treatments did not afford higher yields. The crude cleavage products were treated briefly with DOWEX1-X2 (carbonate form) and gave products of acceptable purity for biological screens (Table 1).

2.1. Mechanistic aspects

The oxadiazole formations were performed with TFAA–CH_2Cl_2–TFA (20:75:5, v/v/v) unless specified otherwise. Under these conditions, three processes were found to occur:

2.1.1 oxadiazole formation on resin,
2.1.2 deacylation of R^1COOH versus cyclization,
2.1.3 sequestration of support-bound species by the resin.

2.1.1. Oxadiazole formation on resin. Scheme 3 shows the TFAA-mediated dehydration of immobilized 2-acyl hydrazides. The TFAA-mediated dehydration of resin-bound diacylhydrazides occurred without dissociation of the 2-acyl hydrazides from the solid support as evidenced by the fact that product mixtures were different from those obtained in solution phase under identical conditions. Specifically, the dehydration of immobilized 2-acyl hydrazide **6a** with TFAA liberated only **7a** and **11a**. Alternatively, the TFAA treatment of compound **8a** in solution phase generated products **7a**, **11a**, and **14** (Scheme 4). In fact, trifluoromethylated oxadiazoles, such as **14**, were never observed in either of our oxadiazole formations involving support-bound 2-acyl hydrazides, or in that involving the *N*-benzylated 2-acyl hydrazide **18** (Scheme 9).

Furthermore, the acidity of CH_2Cl_2–TFA (95:5, v/v) in the absence of dehydrating agents was found to be insufficient to liberate hydrazide **8a** from resin **6a**.

Table 1

Entry	Polymer supported hydrazides	R^1	Acylation method[a]	R^2	R^2COX	Diacyl-hydrazine	Oxadiazoles[b]	Yield[c]	Purity[d]
1	**4a**		A		**5a**	**6a**	**7a**	48	92.5
2	**4a**		B		**5b**	**6ab**	**7b**	63	94.6
3	**4a**		A	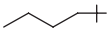	**5c**	**6c**	**7c**	69	96.6
4	**4a**		B	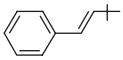	**5d**	**6d**	**7d**	11	89.8
5	**4a**		B		**5e**	**6e**	**7e**	29	93.5
6	**4a**		**C**	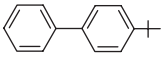	**5f**	**6f**	**7f**	35	96.8
7	**4a**		D	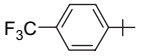	**5g**	**6g**	**7g**	22	100
8	**4a**		D		**5h**	**6h**	**7h**	30	100
9	**4a**		D	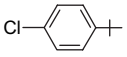	**5i**	**6i**	**7i**	40	87.9
10	**4a**		D	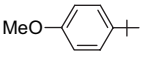	**5j**	**6j**	**7j**	25	79.5
11	**4a**		D		**5k**	**6k**	**7k**	15	80.0
12	**4b**		A		**5a**	**6ba**	**7b**	31	87.2
13	**4b**		D		**5h**	**6l**	**7l**	22	85.1
14	**4c**		A		**5a**	**6m**	**7m**	32	92.3
15	**4c**		C	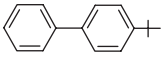	**5f**	**6n**	**7n**	7	91.8
16	**4d**	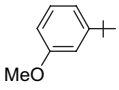	A		**5a**	**6o**	**7o**	49	87.1
17	**4d**	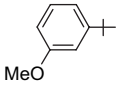	D	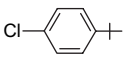	**5i**	**6p**	**7p**	15	79.8
18	**4e**		A		**5a**	**6q**	**7q**	31	88.4

[a] Acylation methods: A: $(R^3CO)_2O$ (0.5 M, 11 equiv), CH_2Cl_2, NMI (0.5 M, 11 equiv), rt 48 h; B: R^3CO_2H (0.5 M, 11 equiv), CH_2Cl_2, NMI (0.025 M, 0.5 equiv), ethoxyacetylene (0.5 M, 11 equiv), rt 48 h; C: (a) R^3CO_2H (0.5 M, 11 equiv), CH_2Cl_2, NMI (1 M, 22 equiv), *i*PrOCOCl (0.5 M, 11 equiv), rt 30 min, (b) addition to resin, rt 48 h; D: (a) R^3COCl (0.5 M, 11 equiv), CH_2Cl_2, NMI (1 M, 22 equiv), pentafluorophenol (PFP) (0.5 M, 11 equiv), rt 30 min, (b) addition to resin, rt 48 h.

[b] All cyclative cleavages were performed using TFAA–CH_2Cl_2–TFA (20:75:5, v/v/v), 5 h, rt.

[c] Isolated yields based on the manufacturer's specification of loading of the initial aldehyde resin (i.e., over four consecutive steps). The crude cyclization product mixture was treated for 3 h with DOWEX1-X2 (carbonate form) before it was isolated and the yields determined by weight.

[d] The purity of the isolated products was determined by integration of the product peak analytical HPLC trace at 220 nm.

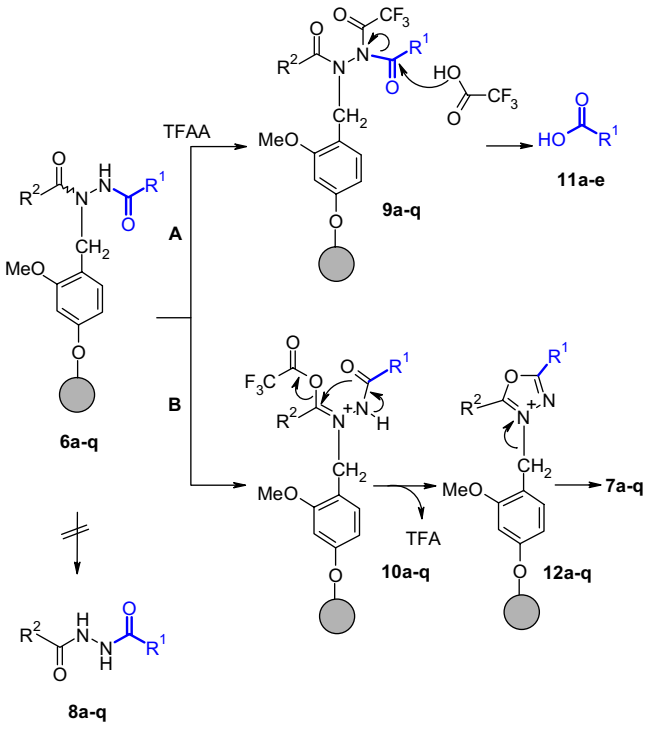

Scheme 3. TFAA-mediated dehydration of solid phase bound 2-acyl hydrazides.

Recent reports on the synthesis of oxadiazolinium salts by analogous dehydration reactions[12] strongly suggest the intermediacy of a support-bound oxadiazolinium species like **12a** (Scheme 3, path B).

The difference in the reaction mechanism between dehydrations in solution and on solid phase is supported by the different impact of the reaction solvent on the product compositions. In solution phase, the ratio of **7a**/**14** was highly solvent dependent (Table 4). On solid phase, the dehydration cocktail had little influence on the product composition. In solution phase, compounds **14** could only have been liberated upon fragmentation of a *N*-trifluoroacylated intermediate, such as **13** (Scheme 4, path A′).

2.1.2. Deacylation R^2COOH versus cyclization. The liberation of acyl groups, such as **11a**, also occurred from a resin-bound species. Here again, resin involvement was evident, since only the acyl groups β to the support-link R^1CO_2H, such as **11a**, were released from the resin (Table 2, Scheme 3, path A). The absence of deacylation in the dehydration reactions using $SOCl_2$ (Table 3) supported the role of a trifluoroacetylated intermediate, such as **9a** (Scheme 3, path A). The deacylation site was determined in a study using the following support-bound hydrazides (Table 2).

We obtained further evidence for the proposed transacylation step[13] (Scheme 3, path A, Scheme 4, path A′) through a solution phase model reaction. When treating benzohydrazide (**2a**) with excess TFAA, we obtained benzoate (**11a**),

Table 2

Entry	Hydrazide resin starting material	Resin-bound 2-acyl hydrazide	Desired oxadiazole (yield %)[a]		Co-isolated acid R^1CO_2H (yield %)[a]	
1	**4a**	**6a**	**7a**	(32.6)	**11a**	(62.2)
2	**4c**	**6m**	**7m**	(68.3)	**11c**	(19.8)
3	**4d**	**6o**	**7o**	(42.5)	**11d**	(41.4)
4	**4e**	**6q**	**7q**	(23.5)	**11e**	(51.6)
5	**4a**	**6d**	**7d**	(37.4)	**11a**	(33.1)

Deacylation of the acyl group 'β' to the support link R^1 during oxadiazole formations on solid support using TFAA–CH_2Cl_2 (1:4, v/v). The acids stemming from R^2 were not observed.

[a] The yields were based on the integration of the product peak in the HPLC trace of the purified product at 220 nm.

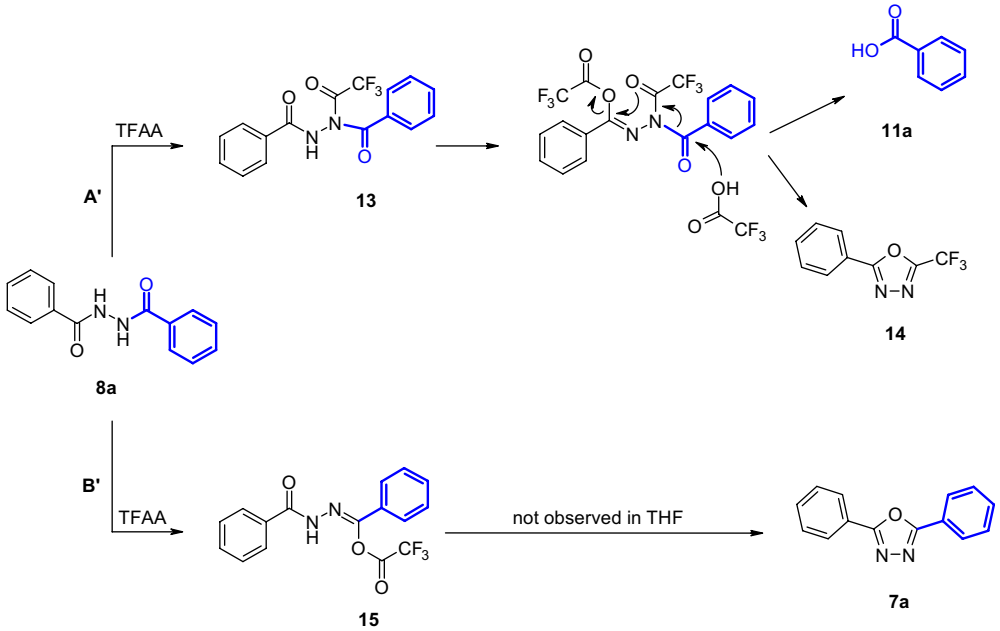

Scheme 4. TFAA-mediated oxadiazole formations in solution phase.

Table 3. $SOCl_2$-mediated oxadiazole formations

Entry	Hydrazide resin starting material	Resin-bound acyl hydrazide	Desired oxadiazole (yield %)[a]		Formed hydrazide (major side product)		
					(yield %)[a]		ESI-MS *m/z* $(M+H)^+$
1	**4a**	**6a**	**7a**	(50.4)	**8a**	(16.8)	241
2	**4b**	**6b**	**7b**	nd[b]	—	nd[b]	—
3	**4c**	**6m**	**7m**	(44.7)	**8m**	(13.2)	259
4	**4d**	**6o**	**7o**	(47.8)	**8o**	(11.8)	271
5	**4e**	**6q**	**7q**	(32.2)	**8q**	(22.4)	247

Oxadiazole formation in $SOCl_2$–CH_2Cl_2–DMF (100:400:1, v/v/v), rt, 15.5 h (126 equiv $SOCl_2$). Deacylation of the acyl group 'β' to the support link R^1 was not observed. Compounds **8a–s** were not observed in TFAA-mediated cyclizations.

[a] The yields were based on the integration of the product peak in the HPLC trace of the crude reaction mixture at 220 nm.

[b] Complex mixture.

and the *O*-trifluoroacetates **X** and **XI**. The calculations were performed using B3LYP[16] density functions with a 6-31G* basis set starting from the MMFF conformer. Among the four hydrazide conformers, the MMFF force field favored **IXa**, **IXc**, and **IXd** while **IXb** was converted into **IXc** upon the optimization. On the bases of earlier calculations and X-ray structures of related compounds,[14,15] conformer **IXc** would clearly be favored. **IXa**, is an 'unusual' conformer with a non-planar amide bond, and is probably an artifact of the calculations.

The calculations suggested the conformers **IXc** (EZ) or **IXd** (EE) to be attacked on the carbonyl functions next to R^2 by dehydrating agents due to the co-localization of their HOMOs and negative charge. Scheme 7 represents a mechanistic pathway elaborating upon the discussions of Scheme 3, considering the results of the MO calculations. The resulting cationic Vilsmeier–Haack intermediate **XI** (Scheme 7)

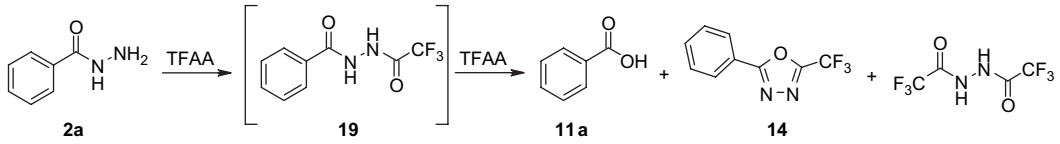

Scheme 5.

oxadiazole **14**, and 2,2,2-trifluoro-*N*′-(trifluoroacetyl) acetohydrazide (Scheme 5).

Unlike with dehydrations involving TFAA, $SOCl_2$-mediated oxadiazole formations were *not* accompanied by deacylation. However, these sluggish reactions yielded oxadiazoles and hydrazides **8a–q** with $M=(M_{oxadiazole}+18)$ (Table 3). Since, $SOCl_2$ is unable to form a stable N-adduct with hydrazides, we deduced N-trifluoroacetylation to be the reason for the deacylation.

A problem with TFAA-mediated oxadiazole formations was the competition with deacylation. In order to gain further insight in the reaction mechanisms, we performed MO calculations on model structures resembling the support-bound intermediates. Based on crystal structures of *N*2-acyl hydrazides[14] and steric bulk imposed by the linker, we assumed the secondary amide to be predominantly in the *Z*-configuration, while the tertiary amide with the support link was assumed to be *E* or *Z*. It is likely that in the support-bound hydrazides, the CO–N–N–CO dihedral angles are near 90° in their lowest energy conformations and the rotation about the N–N bond is hindered ($E_a \approx 19$ kcal/mol).[15]

We performed MO calculations on simplified model hydrazides **IXa** (ZZ), **IXb** (ZE), **IXc** (EZ), **IXd** (EE) (Scheme 6)

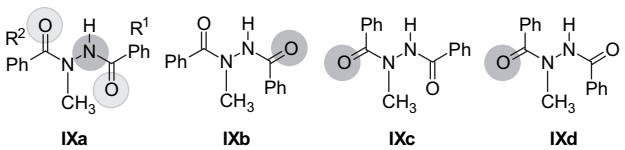

Scheme 6. Structures of the model compounds **IXa–d**. The highlighted atoms indicate the localization of the HOMO.

would initiate oxadiazole formation (as seen in path B, Scheme 3). In turn, an attack of TFAA on the carbonyl functions next to R^1 would lead to the intermediate **X**. This intermediate may not only be a precursor for oxadiazole formation (Scheme 7), but also may initiate deacylation according to path A in Scheme 3. Our calculations suggested the highlighted N atom of **X** to be its most nucleophilic moiety (Schemes 6 and 7). It also may be trifluoroacetylated, initiating path A in Scheme 3. Addition of TFA, as in our preferred cyclization cocktail, may in fact 'protect' the intermediate **X** from N-acylation and promote oxadiazole formation. Indeed, adding TFA to the cyclization cocktail resulted in slightly higher yields.

On the resin, the dehydrating agent TFAA may either attack the more nucleophilic carbonyl function or the more accessible one. It remained difficult to ascertain the influence of the hydrazide conformation on this attack. Attempts to use various NMR methods to determine the conformation of resin-bound hydrazides, such as **6a**, and model compound **18** were unsuccessful.

To support the reaction mechanism on the solid phase (Scheme 3), we also attempted to analyze the chemical species remaining on the polymer after the oxadiazole formation. Unfortunately, the structure of the resins was modified by the TFAA treatment, rendering it impossible to obtain MAS NMR spectra of the remaining resin-bound chemical entities. However, we performed elemental analysis on the resins affording **7a** or **7b** *after* the TFAA treatment. The measured N content of 2.5% was significantly higher than the calculated 1.2% required for the one resin-bound nitrogen, being part of the spacer (Scheme 3). Thus, about 50% of the originally support-bound hydrazide was not involved in oxadiazole formation,

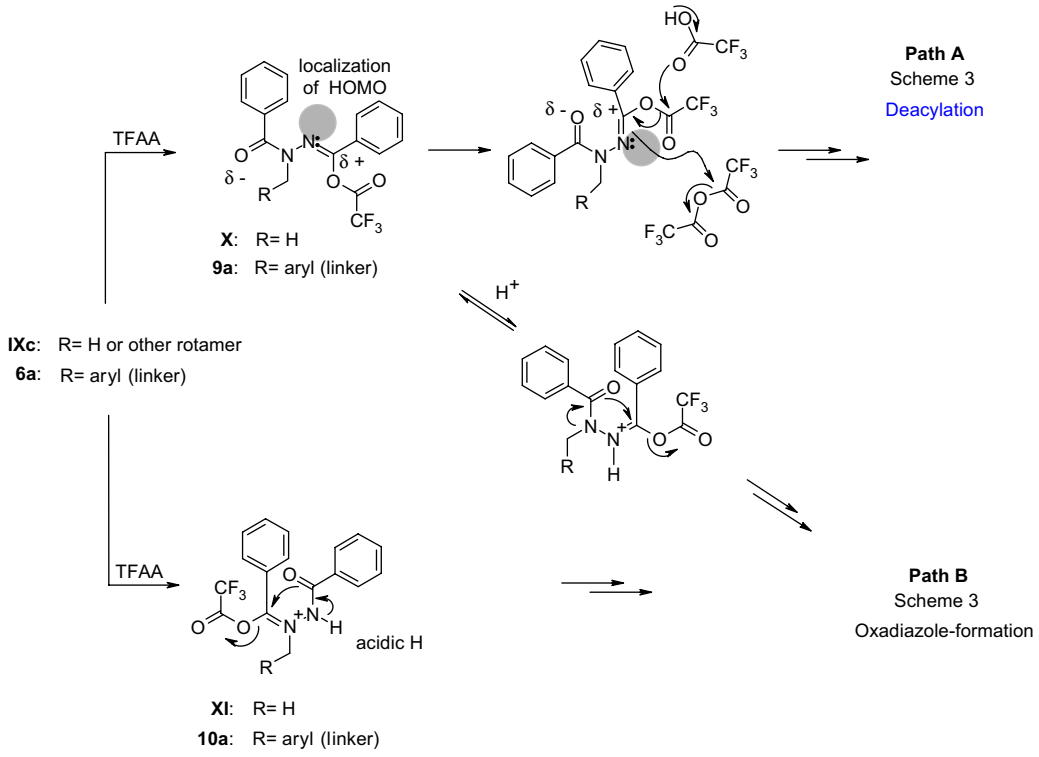

Scheme 7. The expected reactivities of the model structures **IXc**, **X**, and **XI**, corresponded to the proposed intermediates **6a**, **9a**, and **10a**. The highlighted atoms indicate the localization of the HOMO.

and its nitrogen remained on the resin, as suggested by Scheme 3.

Finally, compound **18**, synthesized according to Scheme 8, served as our model for the transformations undergone by the resin-bound hydrazide **6a** during the TFAA treatment.

Fortunately, solution-phase oxadiazole formation using model compound **18** (Scheme 9) afforded the products suggested by reaction pathways A and B in Scheme 3.

Thus, TFAA treatment of compound **18** gave the desired product **7a**. The side products **11a**, **19**[17] ($(M-H)^-$=231), and **20** ($(M+H)^+$=383, $M-H)^-$=381) resulted from the deacylation according to the mechanism in Scheme 3. The deacylation mechanism was further supported by the fact that in the HPLC trace of the reaction mixture at 220 nm, the integration of the peak of **11a** amounted to that of peaks **19** and **20** together. Unlike in TFAA-mediated oxadiazole formations on solid support, we also observed some dibenzoylation of **18**, giving **8a**.

Many lipophilic, high-molecular-weight compounds (M>700), and a white solid, a degradation product of **20**, insoluble in DMSO, DMF, CH_3OH, and water, were observed. Conversely, from the solid phase synthesis, side products **19**, **20**, the several lipophilic side products and the 'white solid' did not elute from the resin, even after repeated TFAA treatment. They remained tightly bound to the support lowering the overall recovery of isolated products. This sequestration by the polymeric support will be discussed in Section 2.1.3.

We also examined the influence of solvents on the outcome of the TFAA-mediated oxadiazole formations. Encouraged by dramatically different **7a**/**14** ratios in solution phase reactions (Table 4), we hoped to find solvents that could suppress the deacylation effectively on solid phase.

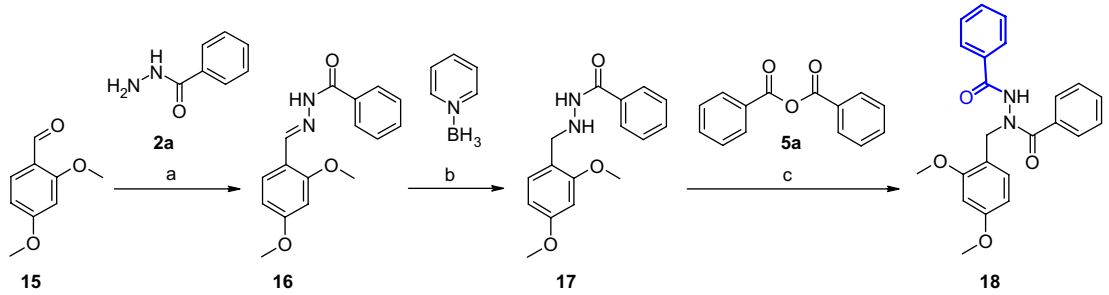

Scheme 8. Reagents and conditions: (a) HOAc, CH_2Cl_2, 24 h, rt; (b) CH_2Cl_2–HOAc (9:1, v/v), 3 h, rt; (c) NMI, CH_2Cl_2, 3 days, rt.

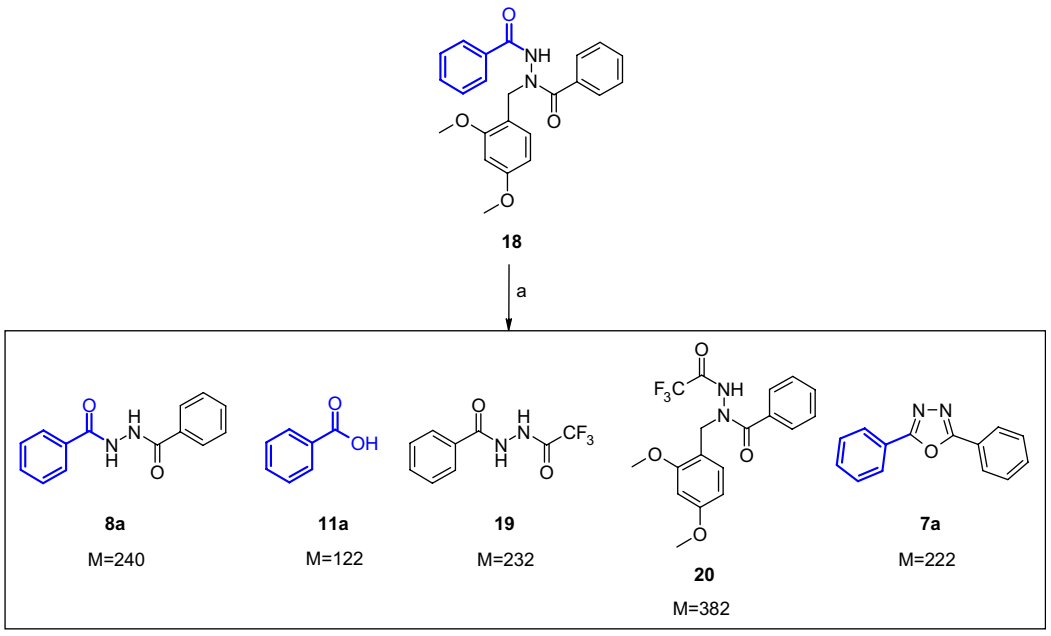

Scheme 9. Reagents and conditions: (a) TFAA–CH_2Cl_2–TFA (20:75:5, v/v/v), 3 h, rt.

Unfortunately, on the solid support, the formation of **7a** could not be improved dramatically by changing reaction solvents.

The reason for the dramatic solvent dependence in TFAA-mediated solution-phase oxadiazole formations is not understood. Our calculations suggested the oxadiazole formation to be a largely charge driven process. In our hands reactions in toluene and THF were much slower than reactions in CH_2Cl_2, which solubilizes ionic intermediates much better. For instance, in the reaction in toluene (Table 4, entry 5) only 3% of the starting material was converted **7a**. The *N*-trifluoroacetyl derivative **19** failed to cyclize at all.

Reaction cocktails containing TFA or ethylene glycol gave broad ^{19}F NMR signals indicating rapid trans-trifluoroacetylation. These cocktails influenced the **7a/14** ratios in solution dramatically, but gave relatively modest effects on solid support. Unfortunately, the influence of the solvent can only be exploited for the reactions on solid phase within limits restricted by use of certain volatile solvents, permitting swelling of the resin and facile product isolation.

Table 4. Solvent influence on oxadiazole formation

Entry	Conditions	Solution phase:ratio[a] **7a**:**14**	Solid phase:isolated yield of **7a**
1	TFAA–THF (1:4)	Only **14**	n.d.
2	TFAA–THF (1:4)+5% TFA	Only **14**	n.d.
3	TFAA–DCM (1:4)+0.1% ethylene glycol	1:7.3	30.2
4	TFAA–DCM (1:4)+5% TFA	64:1	47.9
5	TFAA–toluene (1:4)	Only **7a**[b]	n.d.

[a] The ratio was determined by HPLC/MS at 254 nm after 48 h.
[b] After 48 h HPLC/MS at 220 nm indicated only 3% conversion to **7a**, main products: **8a** (12%), benzoyl hydrazide (41%), and **19** (5%).

2.1.3. Sequestration of support-bound species by the resin. The mass of all isolated products in our oxadiazole formations amounted to less than that was expected, based on the previously discussed pathways A and B (Scheme 3). In our solution phase model, the formation of the uncharacterized 'insoluble white solid' gave additional evidence of a third, 'sequestration pathway'. The latter is independent of TFAA, but mediated by acids. Thus, pre-incubation of resin **6q** with 5% TFA in CH_2Cl_2, prior to addition of TFAA, had an impact on the mass of isolated products (recovery) and on their purity (Fig. 1).

The purity of the isolated products was determined by integration of the product peak of their analytical HPLC traces at 220 nm. The product mixtures contained two components **7q** and **11e**.

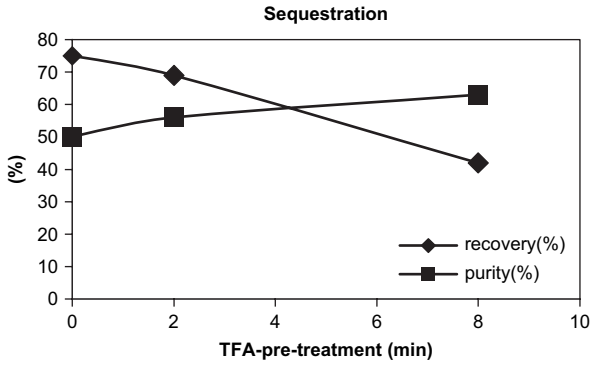

Figure 1. Sequestration of support-bound oxadiazole precursors upon action of TFA on support **6q** for various time periods. Subsequent oxadiazole formation was performed for 5 h in TFAA–CH_2Cl_2–TFA (20:75:5, v/v/v). The recovery was determined by the following equation:

$$\text{recovery}[\%] = \frac{\text{gross isolated mass}}{\text{theoret. yield of oxadiazole}} \times 100.$$

Some dehydrating conditions promote the sequestration of the hydrazide more than others. For support **6a** sequestration follows the order: TFAA–CH_2Cl_2–TFA (20:75:5, v/v/v)<$SOCl_2$–CH_2Cl_2 (25:75, v/v), rt≈$SOCl_2$–$CHCl_3$ (25:75, v/v) 60 °C,<$BF_3\cdot OEt_2$–$CHCl_3$ (1:9, v/v) 60 °C. In the latter case, no oxadiazole could be recovered from the resin. Slow addition of TFAA to a suspension of resin **6q** in CH_2Cl_2 to afford a solution of TFAA–CH_2Cl_2 (20:80, v/v) within 10 h also led to complete sequestration of all products. Though the mechanism of sequestration is not known, it certainly competed with deacylation and oxadiazole formation. Thus, the conditions for oxadiazole formation in Table 1 represent a compromise between purity of the crude desired product and its recovery.

3. Limits

The TFAA-mediated cyclizations were not successful for ureas and thioureas stemming from R^2–NCS or R^2NCO and R^2 bearing aromatic nitro-groups, or α-keto-groups. Chloromethyl oxadiazoles were identified in crude reaction mixtures involving chloroacetylated support-bound hydrazides, but did not survive the methanolic DOWEX-workup due to methoxylation.

4. Conclusion

We have studied the possibility of applying an acid labile linker as a leaving group in the synthesis of 1,3,4-oxadiazoles on solid phase. We also elucidated the role of TFAA in such processes, demonstrating its diverse reactivity. Many oxadiazoles have been obtained in purities suitable for our chemical collection without HPLC purification. In the underlying cyclizations, the linker is really traceless, leaving only an electron pair on the released substrate. Our process of few manipulations makes use of widely available and cheap commercial reagents. However, in order to obtain high isolated yields, other dehydrating conditions and different support linkers would be of need. The dehydrating volatile agent 'TFAA' also imposed some limitations regarding side reactions on choice of building blocks (for instance incompatibility with nitro-groups). In the case of the oxadiazole formation, we have demonstrated the role of the polymeric support in mediating a reaction pathway on solid phase differing from that in solution. The newly discovered reactivity of *N*-benzylated *N′*-acyl hydrazides may be exploitable for other applications.

5. Experimental

5.1. General

4(4-Formyl-3-methoxyphenoxy)butyryl resin was purchased from Calbiochem-Novabiochem AG, Weidenmattweg 4, CH-4448 Laeufelfingen, Switzerland. All solvents and reagents were purchased from Sigma–Aldrich Chemical Company, Inc., 1001 West Saint Paul Avenue, Milwaukee, WI 53233, USA and Dr. Theodor Schuchardt & Company, Edward-Buchner Strasse 14-20, D-85662 Hohenbrunn, Germany. All other solvents and reagents were purchased from Aldrich.

5.1.1. Parallel reactions. Parallel reactions on solid supports were performed in Mettler Bohdan Miniblock: Mettler-Toledo Bohdan Inc., 562 Bunker Court, Vernon Hills, IL 60610 USA.

For the reactions performed on beads, quantitative loading of the resin-bound starting material was assumed. Large excess of reagents was generally applied to assure pseudo-first-order kinetics.

5.1.2. HPLC. HPLC/MS was performed on a Waters XTerra RP18 (4.6×50 mm, 3.5 μm) column using a Waters 2790 HPLC system equipped with a 996 Waters PDA detector and a Micromass mod. ZQ single quadrupole mass spectrometer, equipped with an electrospray (ESI) ion source. Mobile phase A: NH_4OAc (5 mM buffer with HOAc, pH 5.5)–CH_3CN (95:5, v/v); mobile phase B: H_2O–CH_3CN (5:95, v/v). A linear gradient was run from 10 to 90% B in 8 min, hold 90% B 2 min. UV detection at 220 and 254 nm. Flow rate: 1 mL/min; injection volume: 10 μL. Full scan, mass range from 100 to 800 amu. Capillary voltage: 2.5 kV; source temperature: 120 °C; cone voltage: 10 V. Retention times are given in minutes at 220 or 254 nm.

5.1.3. Exact mass. Exact mass data ESI(+) were obtained on a Waters Q-T of Ultima directly connected with micro HPLC 1100 Agilent as previously described.[18]

A reserpine solution 250 pg/μL (about 100 counts/s) was used as a reference compound for TOF Lock Mass correction ($[M+H]^+$ ion 609.2806 *m/z*).

5.1.4. NMR. NMR experiments were performed on two different instruments; chemical shifts were referenced with respect to the residual solvent signals.

^1H NMR spectra were recorded in DMSO-d_6 at a constant temperature of 25 °C on a Varian INOVA 500 spectrometer operating at 499.7 MHz for ^1H. The instrument was equipped with a *Z*-axis gradient triple resonance ^1H {$^{13}C/^{15}N$} PFG ID cold probe.

5.1.4.1. Magic angle spinning NMR. ^1H MAS NMR was performed in DMF-d_7 on a Varian INOVA 500 spectrometer operating at 500.25 MHz for ^1H equipped with a gHX Nano-Probe ($^1H\{^{31}P–^{15}N\}$).

5.1.5. MO calculations. MO calculations were performed using the 'Titan' molecular modeling program by Wavefunctions, Inc. 18401 Von Karman Avenue, Suite 370, Irvine, CA 92612, USA and Schroedinger, Inc. 1500 SW First Avenue, Suite 1180, Portland, OR 97201, USA.

5.2. Hydrazones bound on 4(4-formyl-3-methoxyphenoxy)butyryl resin

To 3-methoxy-benzaldehyde-resin (**1**) (2000 mg, loading 0.86 mmol/g), suspended in CH_2Cl_2 (20 mL), HOAc (1.58 mmol, 100 μL, 0.98 equiv), were added hydrazides

2a–e (1.5 equiv). The slurries were agitated for 18 h at rt, then washed successively with alternating washes of 3× (a) CH_2Cl_2, (b) dioxane; 3× (a) CH_2Cl_2, (b) EtOEt then with 3×EtOEt. The resins were dried in vacuo and analyzed by IR and NMR.

Note: The elemental analysis of resins is not very exact, due to residual solvent. It is an approximation of the loading. All following NMR experiments revealed quantitative conversion.

5.2.1. Resin 3a. IR (powder): 3025, 2972, 2920, 2850, 1645, 1601, 1546, 1503, 1492, 1451, 1420, 1352, 1308, 1272, 1200, 1163, 1115, 1074, 1028, 976, 909, 873, 834, 795, 757, 696 cm^{-1}; ^1H MAS NMR (500 MHz, DMF-d_7) δ 11.86 (1H, NH, hydrazone), 8.90 (1H, CH═N, hydrazone), 8.09 (2H, benzoyl), 7.96 (1H, linker), 7.41–7.57 (3H, benzoyl), 6.67, 6.62 (2H, linker), 4.38 (2H, –NH–CH_2– spacer), 4.10 (2H, –CH_2–O– spacer), 3.83 (3H, Me, linker), 2.49 (2H, –$COCH_2$– spacer), 2.11 (2H, –CH_2– spacer); determination of loading by elemental analysis: N: 3.86%, 0.91 mmol/g.

5.2.2. Resin 3b. IR (powder): 3058, 3025, 2924, 1651, 1601, 1549, 1493, 1452, 1420, 1372, 1309, 1272, 1199, 1163, 1113, 1029, 974, 905, 833, 755, 697 cm^{-1}; ^1H MAS NMR (500 MHz, DMF-d_7) δ 11.53, 11.12 (1H, NH, hydrazone), 8.47, 8.62 (1H, CH═N, hydrazone), 7.90, 7.84 (1H, linker), 7.16–7.45 (5H, phenyl), 6.67–6.70 (2H, linker), 4.39 (2H, NH–CH_2– spacer), 4.10 (2H, –CH_2–O– spacer), 4.06, 3.63 (2H, CH_2), 3.81 (3H, Me, linker), 2.49 (2H, CO–CH_2–O– spacer), 2.12 (2H, –CH_2– spacer); determination of loading by elemental analysis: N: 3.83%, 0.91 mmol/g.

5.2.3. Resin 3c. IR (powder): 305, 2972, 2925, 2851, 1647, 1600, 1586, 1549, 1503, 1493, 1452, 1420, 1359, 1310, 1270, 1200, 1163, 1114, 1029, 961, 907, 817, 799, 748, 697 cm^{-1}; ^1H MAS NMR (500 MHz, DMF-d_7) δ 12.41, 11.88 (1H, NH, hydrazone), 9.14, 8.88 (1H, CH═N, hydrazone), 7.94, 7.87, 7.55, 7.37 (5H, 4H: 3-fluoro benzoyl, 1H: linker), 6.69, 6.63 (2H, linker), 4.39 (2H, –NH–CH_2– spacer), 4.10 (2H, –CH_2–O– spacer), 3.84 (3H, Me, linker), 2.49 (2H, –$COCH_2$– spacer), 2.11 (2H, –CH_2– spacer); determination of loading by elemental analysis: N: 3.67%, 0.89 mmol/g; F: 2.03%, 1.07 mmol/g.

5.2.4. Resin 3d. IR (powder): 3057, 3025, 2923, 1645, 1599, 1544, 1491, 1451, 1420, 1357, 1273, 1199, 1163, 1114, 1030, 973, 908, 972, 804, 747, 697 cm^{-1}; ^1H MAS NMR (500 MHz, DMF-d_7) δ 12.38, 11.82 (1H, NH, hydrazone), 9.06, 8.88 (1H, CH═N, hydrazone), 7.94 (1H, linker), 7.66, 7.41, 7.12 (4H, 3-methoxybenzoyl), 6.58–6.69 (2H, linker), 4.38 (2H, –NH–CH_2– spacer), 4.10 (2H, –CH_2–O– spacer), 3.82 (6H, 3H: Me, linker, 3H: Me, 3-methoxybenzoyl), 2.49 (2H, –$COCH_2$– spacer), 2.11 (2H, –CH_2– spacer).

5.2.5. Resin 3e. IR (powder): 3034, 2922, 1641, 1600, 1550, 1505, 1551, 1493, 1451, 1417, 1377, 1309, 1272, 1223, 1200, 1163, 1113, 1030, 975, 908, 826, 756, 732, 697 cm^{-1}; ^1H MAS NMR (500 MHz, DMF-d_7) δ 11.88, 11.56 (1H, NH, hydrazone), 8.82, 8.60 (1H, CH═N, hydrazone), 8.17, 7.85 (1H, H3, thienyl), 8.06, 7.80 (1H, 1H: H5, thienyl), 8.06, 7.93 (1H, linker), 7.17 (1H, H4, thienyl), 6.55–6.73 (2H, linker), 4.39 (2H, –NH–CH_2– spacer), 4.12 (2H, –CH_2–O– spacer), 3.84 (3H, Me, linker), 2.49 (2H, –$COCH_2$– spacer), 2.13 (2H, –CH_2– spacer); determination of loading by elemental analysis: N: 3.74%, 0.89 mmol/g, S: 2.31%, 0.79 mmol/g.

5.3. Reduction of resin-bound hydrazones 3a–e to hydrazides 4a–e

Hydrazone resins **3a–e** (1000 mg, loading 0.86 mmol/g) were suspended in 10 mL of (CH_2Cl_2–HOAc–pyridine·BH_3 (85:10:5, v/v/v) and agitated for 8 h at rt. The reaction mixtures were washed successively with alternating washes of 3× (a) DMF, (b) CH_2Cl_2; 3× (a) MeOH, (b) CH_2Cl_2; 3× (a) CH_2Cl_2, (b) EtOEt and 3×EtOEt. The resins were dried in vacuo and analyzed by IR and NMR. All following NMR experiments revealed quantitative conversion.

5.3.1. Resin 4a. IR (powder): 1651, 1611, 1506, 1493, 1419, 1284, 1263, 1198, 1160, 1131, 1028, 970, 901, 821, 757, 697 cm^{-1}; ^1H MAS NMR (500 MHz, DMF-d_7) δ 9.97–10.27 (1H, –CO–N*H*–NH–), 7.85–8.03 (2H, *o*-CH, benzoyl), 7.32–7.58 (1H, *p*-CH, benzoyl), 7.03–7.29m (1H, linker), 7.03–7.28 (2H, *m*-CH, benzoyl), 6.54–6.65 (1H, linker), 6.42–6.51 (1H, linker), 4.23–4.53 (2H, –N–CH_2– spacer), 3.9–4.12 (4H, –CH_2–O–, –CH_2–NH–NH– linker), 2.36–2.55 (2H, –$COCH_2$– spacer), 2.03–2.07 (2H, –CH_2– spacer).

5.3.2. Resin 4b. IR (powder): 1662, 1647, 1613, 1506, 1493, 1451, 1419, 1286, 1262, 1197, 1160, 1132, 1031, 971, 829, 756, 679 cm^{-1}; ^1H MAS NMR (500 MHz, DMF-d_7) δ 9.44–9.86 (1H, –CO–N*H*–NH–), 6.82–7.52 (6H, 5H: phenyl, 1H: linker), 6.53–6.60 (1H, 1H, linker), 6.43–6.49 (1H, linker), 4.22–4.50 (2H, –N–CH_2– spacer), 3.45–3.49 (2H, CH_2, benzyl), 3.98–4.13 (4H, –CH_2–O–), 3.83–3.93 (2H, –N–CH_2– spacer), 3.68–3.81 (5H, Me linker, –CH_2–NH–NH– linker), 2.41–2.59 (2H, –$COCH_2$– spacer), 2.06–2.18 (2H, –CH_2– spacer).

5.3.3. Resin 4c. IR (powder): 2920, 1647, 1612, 1585, 1493, 1451, 1420, 1286, 1269, 1199, 1160, 1130, 1030, 972, 942, 888, 820, 795, 754, 697 cm^{-1}; ^1H MAS NMR (500 MHz, DMF-d_7) δ 9.92–10.52 (1H, –CO–N*H*–NH–), 7.76–7.85 (1H, 3-fluorophenyl), 7.68–7.76 (1H, 3-fluorophenyl), 7.16–7.34 (2H, 1H: 3-fluorophenyl, 1H: linker), 6.52–6.64 (1H, linker), 6.41–6.50 (1H, linker), 4.22–4.53 (2H, –N–CH_2– spacer), (2H, –CH_2–NH–NH– linker, –CH_2–NH–NH– linker), 3.91–4.16 (4H, –CH_2–O–, N–CH_2– spacer), 3.61–3.96 (3H, Me, linker), 2.29–2.61 (2H, –$COCH_2$– spacer), 1.99–2.22 (2H, –CH_2– spacer).

5.3.4. Resin 4d. IR (powder): 1653, 1607, 1582, 1539, 1506, 1492, 1451, 1421, 1284, 1198, 1160, 1132, 1119, 1033, 972, 835, 793, 756, 697 cm^{-1}; ^1H MAS NMR (500 MHz, DMF-d_7) δ 9.92–10.33 (1H, –CO–N*H*–NH–), 7.48–7.59 (2H, 3-methoxybenzoyl), 7.29–7.41 (1H, 1H: 3-methoxybenzoyl), 7.21–7.27 (1H, linker), 7.00–7.13 (1H, 3-methoxybenzoyl), 6.53–6.63 (1H, linker), 6.41–6.52 (1H, linker), 4.15–4.52 (2H, –N–CH_2– spacer), 3.92–4.07 (2H, –CH_2–O–), 3.90–4.09 (2H, –CO–NH–NH–CH_2–), 3.67–3.85 (6H, 3H: Me methoxybenzoyl, 3H: Me, linker), 2.41–2.53 (2H, –$COCH_2$– spacer), 2.04–2.17 (2H, –CH_2– spacer).

5.3.5. Resin 4e. IR (powder): 1652, 1613, 1539, 1505, 1493, 1451, 1417, 1286, 1198, 1160, 1127, 1028, 968, 908, 821, 756, 697 cm^{-1}; ^1H MAS NMR (500 MHz, DMF-d_7) δ 9.97–10.26 (1H, –CO–N*H*–NH–), 7.81–7.90 (1H, H5 thienyl), 7.62–7.73 (1H, H3 thienyl), 7.19–7.29 (1H, linker), 7.04–7.15 (1H, H4 thienyl), 6.55–6.63 (1H, linker), 6.43–6.52 (1H, linker), 4.23–4.50 (2H, –N–CH_2– spacer), 3.92–4.12 (4H, 2H: –CH_2–NH–NH– linker, 2H: –$COCH_2$– spacer), 3.66–3.84 (3H, Me, linker), 2.40–2.56 (2H, –$COCH_2$– spacer), 2.09 (2H, –CH_2– spacer).

5.4. Acyl hydrazides

The acyl hydrazides have been isolated as side products during the $SOCl_2$-mediated oxadiazole formation (Table 3). Their mass spectrum and HPLC retention time match that of the reference compounds synthesized in the following way.

5.5. Representative procedure: *N′*-benzoylbenzohydrazide (8a)

To a suspension of benzohydrazide (2 mmol, 272 mg) in CH_2Cl_2, DIEA (2.5 mmol, 424 μL) was added benzoyl chloride (2.1 mmol, 243 μL). A massive precipitation was observed immediately. After 3 h at rt the solid was filtered off and washed with CH_2Cl_2. The white solid was dried in vacuo and analyzed. Yield: 458 mg, 95.3%.

5.5.1. *N′*-Benzoylbenzohydrazide (8a). ^1H NMR (500 MHz, DMSO-d_6) δ 10.50 (2H, s, NH), 7.94 (4H, m, H2, H6 phenyl), 7.62 (2H, m, H4 phenyl), 7.54 (4H, m, H3, H5 phenyl). HRMS *m/z* calcd for $C_{14}H_{12}N_2O_2$: 241.0971 $(M+H)^+$, found 241.0983.

5.5.2. *N′*-Benzoyl-3-fluorobenzohydrazide (8m). ^1H NMR (500 MHz, DMSO-d_6) δ 10.56 (2H, s, NH), 7.93 (2H, m, H2, H6 phenyl), 7.74–7.81 (m, 2H, H2, H6 3-fluorophenyl), 7.61 (2H, m, H4 phenyl, H5 3-fluorophenyl), 7.54 (2H, m, H3, H5 phenyl), 7.51 (1H, m, H4 3-fluorophenyl).

5.5.3. *N′*-Benzoyl-3-methoxybenzohydrazide (8o).[19] ^1H NMR (500 MHz, DMSO-d_6) δ 10.50 (2H, s, NH), 7.94 (2H, m, H2, H6 phenyl), 7.61 (m, 1H, H4 phenyl), 7.38–7.57 (m, 5H, H4, H5, H6 3-methoxyphenyl, H3, H5 phenyl), 7.19 (1H, m, H2 3-methoxyphenyl), 3.82, 3.84 (3H, 2s, Me).

5.5.4. *N′*-Benzoylthiophene-2-carbohydrazide (8q). ^1H NMR (500 MHz, DMSO-d_6) δ 10.50 (2H, s, NH), 7.94 (4H, m, H2, H6 phenyl, H3, H5 thienyl), 7.54 (3H, m, H3, H4, H5 phenyl), 7.23 (1H, m, H4 thienyl), HRMS *m/z* calcd for $C_{12}H_{10}N_2O_2S$: 247.0536 $(M+H)^+$, found 247.0546.

5.6. Solution-phase synthesis of 2-phenyl-5-(trifluoromethyl)-1,3,4-oxadiazole (14)

To **8a** (220 mg, 0.5 mmol) was added a solution of THF–TFAA (4:1, v/v) (5 mL). The reaction mixture became homogeneous after 5 min, though the TLC of an aliquot of the hydrolyzed reaction mixture did not indicate any conversion. The reaction mixture was stirred at rt for another 3 days. The TLC of the reaction mixture then revealed complete conversion into two products. CH_2Cl_2–MeOH (9:1, v/v) R_f: 0.78, 0.38. The reaction mixture was poured on ice and was extracted with CH_2Cl_2. The organic phase was dried over Na_2SO_4, the salts were removed, and the crude product was chromatographed on silica using CH_2Cl_2–MeOH (95:5, v/v).

The high R_f product (105 mg, 97.6%) was **14**. ^1H NMR (300 MHz, $CDCl_3$) δ 8.10–8.13 (2H, d, H2, H6 phenyl), 7.53–7.66 (3H, m, H3, H4, H5 phenyl), (ESI-MS) *m/z*: 215.0 $(M+H)^+$, 232.1 $(M+NH_4)^+$. The low R_f product was benzoic acid **11a**: (ESI-MS) 121.1 $(M-H)^-$.

5.7. Acylated resins

On-bead acylations were performed in Bohdan Miniblocks® on 50 mg of reduced resins (**4a–e**) per reactor. To this amount of resin was then added 2 mL of an acylating solution.

The following solutions were used:

A: To a reactor was added 2 mL of a solution of $(R^2CO)_2O$ (0.5 M), NMI (0.5 M) in CH_2Cl_2.

B: To a reactor were added R^2CO_2H (1 mmol), *N*-methyl imidazole (0.025 mmol), CH_2Cl_2 (2 mL), and ethoxyacetylene (1 mmol as solution in hexane, quantity based on the titer).

C: In an oven dried glass vial, covered with a septum was made a solution (or suspension) of R^2CO_2H (1 M) in CH_2Cl_2 to which was added 2 M equiv of *N*-methyl imidazole. The resulting solution was cooled to 0 °C, and 1 M equiv of isopropyl chloroformate was added as 1 M solution in toluene. The resulting reagent was allowed to come to rt within 30 min and was then added (2 mL per each reactor) to the corresponding reactors in the Miniblock using a syringe.

D: In an oven dried glass vial closed with a septum a solution of pentafluorophenol (PFP) (0.5 M, 1 equiv) and *N*-methyl imidazole (1 M, 2 equiv) in CH_2Cl_2 was prepared. To the resulting solution 1 M equiv (based on PFP) of R^2COCl was added at 0 °C. The resulting solution was allowed to come to rt within 30 min and was then added (2 mL per each reactor) to the corresponding reactors in the Miniblock using a syringe.

The resins were agitated in an orbital shaker for 48 h and were washed using 3×DMF (2 mL) and 1×DMF–H_2O–NEt_3 (4:1:1, v/v/v) (2 mL), followed by alternating washes with 3× (a) DMF (2 mL), (b) CH_2Cl_2 (2 mL); 3× (a) MeOH (2 mL), (b) CH_2Cl_2 (2 mL); 3× (a) CH_2Cl_2 (2 mL), (b) Et_2O (2 mL); 3×Et_2O.

The resins were dried in vacuo for 5 h prior to the cyclative oxadiazole formation.

The following resins were analyzed on solid phase. (Attempted cleavage of the acylated resins with TFA gave complex mixtures, which could not be used for analysis of the resin.) All following NMR experiments revealed quantitative conversion!

5.7.1. Resin 6a. ^1H MAS NMR (500 MHz, DMF-d_7) δ 10.93 (1H, –CO–N*H*–), 7.69 (4H, H2, H6 benzoyl), 7.42 (1H, H4

benzoyl on *tert* amide), 7.31 (1H, H6 linker), 7.12 (5H, H3, H4, H5 benzoyl on primary amide, H3, H5 on secondary amide), 6.59 (1H, H3 linker), 6.51 (1H, H5 linker), 5.51, 4.42 (2H, CH_2, linker), 4.05 (2H, –CH_2–O– spacer), 3.73, 3.64 (3H, Me, linker), 2.47 (2H, –$COCH_2$– spacer), 2.09 (2H, –CH_2– spacer).

5.7.2. Resin 6ba. ^{1}H MAS NMR (500 MHz, DMF-d_7) δ 10.57 (1H, –CO–N*H*–), 7.54 (2H, H2, H6 benzoyl), 7.15–7.39 (6H, H3, H4, H5 benzoyl, H6, linker), 6.91 (2H, H2, H6 benzyl), 6.64 (1H, H3 linker), 6.52 (1H, H5, linker), 5.43, 4.32 (2H, CH_2, linker), 4.09 (2H, –CH_2–O– spacer), 3.77, 3.74 (3H, Me, linker), 2.50 (2H, –$COCH_2$– spacer), 2.13 (2H, –CH_2– spacer).

5.7.3. Resin 6m. ^{1}H MAS NMR (500 MHz, DMF-d_7) δ 11.05 (1H, –CO–N*H*–), 7.69 (2H, H2, H6 benzoyl), 7.56 (1H, H6 3-fluorophenyl), 7.44 (2H, H2, H4 3-fluorophenyl), 7.16–7.34 (2H, 1H: 3-fluorophenyl, H6: linker), 6.61 (1H, H3, linker), 6.54 (1H, H5 linker), 5.50, 4.44 (2H, CH_2 linker), 4.07 (2H, –CH_2–O–, N–CH_2– spacer), 3.66 (3H, Me, linker), 2.49 (2H, –$COCH_2$– spacer), 2.11 (2H, –CH_2– spacer).

5.7.4. Resin 6o. ^{1}H MAS NMR (500 MHz, DMF-d_7) δ 10.91 (1H, –CO–N*H*–), 7.69 (2H, H2, H5 benzoyl), 7.31 (5H, H5, H6 3-methoxybenzoyl, H3, H4, H5 benzoyl, H6 linker), 7.21 (1H, H2 3-methoxybenzoyl), 7.03 (1H, H4 3-methoxybenzoyl), 6.60 (1H, H3, linker), 6.52 (1H, H5 linker), 5.49, 4.41 (2H, CH_2 linker), 4.05 (2H, –CH_2–O), 3.73, 3.70 (3H, Me 3-methoxybenzoyl), 3.66 (3H, Me linker), 2.46 (2H, –$COCH_2$– spacer), 2.04–2.17 (2H, –CH_2– spacer).

5.7.5. Resin 6q. ^{1}H MAS NMR (500 MHz, DMF-d_7) δ 10.95 (1H, –CO–N*H*–), 7.65 (3H, H5 thienyl, H2, H6 benzoyl), 7.27 (1H, H6 linker), 7.01 (1H, H4 thienyl), 6.57 (1H, H3 linker), 6.49 (1H, H5 linker), 5.44, 4.37 (2H, CH_2 linker), 4.03 (2H, –O–CH_2 spacer), 3.60 (3H, Me linker), 2.44 (2H, –$COCH_2$– spacer), 2.07 (2H, –CH_2– spacer).

5.8. Oxadiazole formation on solid phase

The acylated resins were treated with a solution of TFAA–CH_2Cl_2–TFA (20:75:5, v/v/v) (2 mL per reactor) for 5 h at rt. The reaction mixture was drained and the resin was washed with TFAA–CH_2Cl_2–TFA (20:75:5, v/v/v) (1 mL per reactor). The effluent was collected and toluene (1 mL per reaction) was added prior to the evaporation of the reaction mixtures. This toluene addition prevents buildup of TFA and TFAA during the evaporation process, which may lead to side reactions when acids with a –CH_2(C=O)OH– motif are used. The dried reaction mixtures were weighed and analyzed by HPLC/MS to obtain the crude yields. The crude, dried down reaction mixtures were dissolved in MeOH (3 mL each). The resulting solutions were transferred into another Miniblock containing reactors filled with DOWEX1-X2 (carbonate form) (50 mg per reaction). The methanolic solutions of the crude products were agitated for another 3 h prior to filtration and a wash of the DOWEX with methanol (1 mL). The filtrates were analyzed by HPLC/MS for purity and evaporated to white powders or crystals to obtain the isolated yields.

5.9. Analysis of what remained on the resin

Resins **6a** and **6b** were washed after the oxadiazole formation and isolation of the products as follows: 5× with CH_2Cl_2 (2 mL) followed by alternating washes with 3× (a) MeOH (2 mL), (b) CH_2Cl_2 (2 mL); 3× (a) CH_2Cl_2 (2 mL), (b) Et_2O (2 mL); 3×Et_2O. The resins were dried in vacuo for 5 h prior to submission to elemental analysis or ^{1}H MAS NMR (see text, Section 2.1.2).

5.10. Oxadiazoles

5.10.1. 2,5-Diphenyl-1,3,4-oxadiazole (7a). ^{1}H NMR (500 MHz, DMSO-d_6) δ 8.15–8.18 (4H, m, H2, H6 phenyl), 7.63–7.71 (6H, m, H3, H4, H5 phenyl). UV: (λ_{max}) 278 nm; HRMS *m*/*z* calcd for $C_{14}H_{10}N_2O$: 223.0866 $(M+H)^+$, found: 223.0865; HPLC retention time: 6.27 min.

5.10.2. 2-Benzyl-5-phenyl-1,3,4-oxadiazole (7b). ^{1}H NMR (500 MHz, DMSO-d_6) δ 7.96–7.99 (2H, m, H2, H6 phenyl), 7.57–7.66 (3H, m, H3, H4, H5 phenyl), 7.37–7.42 (4H, m, H2, H3, H5, H6 *phenyl*-methyl), 7.29–7.35 (1H, m, H4 *phenyl*-methyl), 4.38 (2H, br s, CH_2, phenyl-methyl). UV: (λ_{max}) 251 nm; HRMS *m*/*z* calcd for $C_{15}H_{12}N_2O$: 237.1022 $(M+H)^+$, found: 237.1032; HPLC retention time: 5.94 min.

5.10.3. 2-Butyl-5-phenyl-1,3,4-oxadiazole (7c). ^{1}H NMR (500 MHz, DMSO-d_6) δ 7.98–8.01 (2H, m, H2, H6 phenyl), 7.59–7.64 (3H, m, H3, H4, H5 phenyl), 2.95 (2H, t, J=8 Hz, α-CH_2, *n*-Bu), 1.77 (2H, m, β-CH_2, *n*-Bu), 1.42 (2H, m, γ-CH_2, *n*-Bu), 0.94 (3H, t, J=8 Hz, Me, *n*-Bu). UV: (λ_{max}) 248 nm, MS (CI) *m*/*z* (relative intensity) 203 ([M+H] 100%), HMRS *m*/*z* calcd for $C_{12}H_{14}N_2O$: 203.1179 $(M+H)^+$, found: 203.1180; HPLC retention time: 5.96 min.

5.10.4. 2-Phenyl-5-[(*E*)-2-phenylvinyl]-1,3,4-oxadiazole (7d). ^{1}H NMR (500 MHz, DMSO-d_6) δ 8.11–8.14 (2H, m, H2, H6 phenyl), 7.81–7.84 (2H, m, H2, H6 phenyl of cinnamyl), 7.80 (1H, d, J=17 Hz, –*H*C=CH–Ph, cinnamyl), 7.61–7.71 (3H, m, H3, H4, H5 phenyl), 7.42–7.51 (3H, m, H3, H4, H5 phenyl of cinnamyl), 7.41 (1H, d, J=17 Hz, –HC=C*H*–Ph, cinnamyl). UV: 253.9, 313.2 nm, HMRS calcd for $C_{16}H_{12}N_2O$: 249.1022 $(M+H)^+$, found: 249.1011; HPLC retention time: 6.82 min.

5.10.5. 2-(2-Methylphenyl)-5-phenyl-1,3,4-oxadiazole (7e). ^{1}H NMR (500 MHz, DMSO-d_6) δ 8.13–8.17 (2H, m, H4, H6 2-methyl phenyl), 8.1 (1H, dd, J=8 Hz, J'=1 Hz, H3 2-methyl phenyl), 7.64–7.70 (3H, m, H2, H6 phenyl, H5 2-methyl phenyl), 7.56 (1H, m, H4 phenyl), 7.41–7.52 (2H, m, H3, H5 phenyl), 2.72 (3H, s, Me). UV: (λ_{max}) 281.1 nm, HRMS *m*/*z* calcd for $C_{15}H_{12}N_2O$: 237.1022 $(M+H)^+$, found: 237.1012; HPLC retention time: 6.91 min.

5.10.6. 2-Biphenyl-4-yl-5-phenyl-1,3,4-oxadiazole (7f). ^{1}H NMR (500 MHz, DMSO-d_6) δ 8.25 (2H, d, J=9 Hz, H2, H6 4-phenyl *phenyl*), 8.17–8.20 (2H, m, H2, H6 phenyl), 7.97 (2H, d, J=9 Hz, H3, H5 4-phenyl *phenyl*), 7.80–7.83 (2H, m, H2′, H6′ 4-*phenyl* phenyl), 7.64–7.69 (3H, m, H3, H4, H5 phenyl), 7.55 (2H, t, J=7 Hz, H3′, H5′ 4-phenyl phenyl), 7.46 (1H, t, J=7 Hz, H4′ 4-phenyl phenyl). UV: (λ_{max}) 301.3 nm, HRMS *m*/*z* calcd for $C_{20}H_{14}N_2O$:

299.1179 $(M+H)^+$, found: 299.1171; HPLC retention time: 8.07 min.

5.10.7. 2-Phenyl-5-[4-(trifluoromethyl)phenyl]-1,3,4-oxadiazole (7g). ^{1}H NMR (500 MHz, DMSO-d_6) δ 8.37 (2H, d, J=9 Hz, H2, H6 trifluoromethyl phenyl), 8.19 (2H, dd, J=8, J'=2 Hz, H2, H6 phenyl), 7.80 (m, 3H, H3, H4, H5 phenyl). UV: (λ_{max}) 282.3 nm, HRMS m/z calcd for $C_{15}H_9F_3N_2O$: 291.0740 $(M+H)^+$, found: 291.0744; HPLC retention time: 7.38 min.

5.10.8. 2-(2-Furyl)-5-phenyl-1,3,4-oxadiazole (7h). ^{1}H NMR (500 MHz, DMSO-d_6) δ 8.08–8.11 (3H, m, H2, H6 phenyl, H3 furyl), 7.62–7.71 (3H, m, H3, H4, H5 phenyl), 7.48 (1H, dd, J=4 Hz, J'=1 Hz, H5 furyl), 6.85 (1H, m, H4, furyl). UV: (λ_{max}) 238.6, 293 nm, HRMS m/z calcd for $C_{12}H_8N_2O_2$: 213.0658 $(M+H)^+$, found: 213.0668; HPLC retention time: 5.32 min.

5.10.9. 2-(4-Chlorophenyl)-5-phenyl-1,3,4-oxadiazole (7i). ^{1}H NMR (500 MHz, DMSO-d_6) δ 8.17 (4H, m, H2, H6 phenyl, H2, H6 4-chlorophenyl), 7.75 (2H, m, H3, H5 4-chlorophenyl), 7.67 (3H, m, H3, H4, H5 phenyl). UV: (λ_{max}) 287.4 nm, HRMS m/z calcd for $C_{14}H_9ClN_2O$: 257.0476 $(M+H)^+$, found: 257.0468; HPLC retention time: 7.12 min.

5.10.10. 2-(4-Methoxyphenyl)-5-phenyl-1,3,4-oxadiazole (7j). ^{1}H NMR (500 MHz, DMSO-d_6) δ 8.13–8.15 (2H, m, H2, H6 phenyl), 8.10 (2H, d, J=8 Hz, H3, H5 4-methoxyphenyl), 7.61–7.68 (m, 3H, H3, H4, H5 phenyl), 7.20 (2H, d, J=8 Hz, H3, H5 4-methoxyphenyl), 3.89 (3H, s, Me). UV: (λ_{max}) 243.3, 294.2 nm, HRMS m/z calcd for $C_{15}H_{12}N_2O_2$: 253.0971 $(M+H)^+$, found: 253.0972; HPLC retention time: 6.31 min.

5.10.11. 2-(1-Naphthyl)-5-phenyl-1,3,4-oxadiazole (7k). ^{1}H NMR (500 MHz, DMSO-d_6) δ 9.21 (1H, d, J=9 Hz, H2 naphthyl), 8.43 (1H, d, J=7 Hz, H8 naphthyl), 8.26 (1H, d, J=7 Hz, H5 naphthyl), 8.21 (2H, m, H2, H6 phenyl), 8.13 (1H, J=9 Hz, H4 naphthyl), 7.65–7.83 (m, 6H (H3, H4, H5 phenyl, H3, H6, H7 naphthyl). UV: (λ_{max}) 222.1, 263.4, 313.2 nm, HRMS m/z calcd for $C_{18}H_{12}N_2O$: 273.1022 $(M+H)^+$, found: 273.1010; HPLC retention time: 7.72 min.

5.10.12. 2-Benzyl-5-(2-furyl)-1,3,4-oxadiazole (7l). ^{1}H NMR (500 MHz, DMSO-d_6) δ 8.03 (1H, m, H5 furyl), 7.29–7.41 (6H, m, phenyl, H3 furyl), 6.78 (1H, m, H4 furyl), 4.36 (2H, s, CH_2–Ph). UV: (λ_{max}) 266.9 nm. MS (CI) m/z (relative intensity) 227 ($[M+H]^+$ 100%), HPLC retention time: 5.97 min.

5.10.13. 2-(3-Fluorophenyl)-5-phenyl-1,3,4-oxadiazole (7m). ^{1}H NMR (500 MHz, DMSO-d_6) δ 8.18 (2H, m, H2, H6 phenyl), 8.01 (1H, m, H6 3-fluorophenyl), 7.99 (1H, m, H2 3-fluorophenyl), 7.64–7.74 (4H, m, H3, H4, H5 phenyl, H5 3-fluorophenyl), 7.55 (1H, t of m, J=9 Hz, H4 3-fluorophenyl). UV: (λ_{max}) 280 nm, HRMS m/z calcd for $C_{14}H_9FN_2O$: 241.0772 $(M+H)^+$, found: 241.0762; HPLC retention time: 6.55 min.

5.10.14. 2-Biphenyl-4-yl-5-(3-fluorophenyl)-1,3,4-oxadiazole (7n). ^{1}H NMR (500 MHz, DMSO-d_6) δ 8.27 (2H, d, J=9 Hz, H2, H6 4-phenyl-*phenyl*), 8.04 (1H, m, H5 3-fluorophenyl), 8.00 (1H, m, H2 3-fluorophenyl), 7.97 (2H, d, 9 Hz, H3, H5 4-phenyl-*phenyl*), 7.82 (2H, d, J=8 Hz, H2′, H6′ 4-*phenyl*-phenyl), 7.72 (1H, m, H5 3-fluorophenyl), 7.53–7.57 (3H, m, H4 3-fluorophenyl, H3′, H5′ 4-*phenyl*-phenyl), 7.47 (1H, t, J=7 Hz, H4′ 4-*phenyl*-phenyl). UV: (λ_{max}) 302.5 nm, HRMS m/z calcd for $C_{20}H_{13}FN_2O$: 317.1085 $(M+H)^+$, found: 317.1088; HPLC retention time: 8.27 min.

5.10.15. 2-(3-Methoxyphenyl)-5-phenyl-1,3,4-oxadiazole (7o). ^{1}H NMR (500 MHz, DMSO-d_6) δ 8.18 (2H, m, H2, H6 phenyl), 7.74 (1H, d of m, J=8 Hz, H6 3-methoxyphenyl), 7.67 (4H, m, H2 3-methoxyphenyl, H3, H4, H5 phenyl), 7.58 (1H, t, J=8 Hz, H5, 3-methoxyphenyl), 7.25 (1H, dd, J=8 Hz, J'=1 Hz, H4, 3-methoxyphenyl), 3.9 (3H, s, Me). UV: (λ_{max}) 280, 313 nm; HRMS m/z calcd for $C_{15}H_{12}N_2O_2$: 253.0971 $(M+H)^+$, found: 253.0962; HPLC retention time: 6.49 min.

5.10.16. 2-(4-Chlorophenyl)-5-(3-methoxyphenyl)-1,3,4-oxadiazole (7p). ^{1}H NMR (500 MHz, DMSO-d_6) δ 8.18 (2H, m, J=9 Hz, H2, H6 4-chlorophenyl), 7.72 (1H, m, H6 3-methoxyphenyl), 7.72 (2H, d, J=9 Hz, H3, H5 4-chlorophenyl), 7.65 (1H, m, H2 3-methoxyphenyl), 7.56 (1H, t, J=8 Hz, H5 3-methoxyphenyl), 7.24 (1H, dd, J=8 Hz, J'=1 Hz, H4, 3-methoxyphenyl), 3.89 (3H, s, Me). UV: (λ_{max}) 236–242 nm (plateau), 283 nm; HRMS m/z calcd for $C_{15}H_{11}ClN_2O_2$: 287.0582 $(M+H)^+$, found: 287.0568; HPLC retention time: 7.03 min.

5.10.17. 2-Phenyl-5-(2-thienyl)-1,3,4-oxadiazole (7q). ^{1}H NMR (500 MHz, DMSO-d_6) δ 8.12 (2H, m, H2, H6 phenyl); 7.98 (2H, m, H3, H5 thienyl), 7.62–7.7 (3H, m, H3, H4, H5 phenyl), 7.36 (1H, m, H4 thienyl). UV: (λ_{max}) 300.7 nm, HRMS m/z calcd for $C_{12}H_8N_2OS$: 229.0430 $(M+H)^+$, found: 229.0425; HPLC retention time: 5.95 min.

5.11. Trans-trifluoroacetylation: reaction of 2a with TFAA

Benzohydrazide **2a** (0.367 mmol, 50 mg) was treated with TFAA–CH_2Cl_2 (1:4, v/v) (2 mL) for 14 h at rt. A white precipitate formed, which was found to be 2,2,2-trifluoro-*N*′-(trifluoroacetyl)acetohydrazide upon comparison with an authentic sample prepared according to Ref. 6a. The crude reaction mixture was taken up in MeCN–H_2O (4:1, v/v) and subjected to HPLC/MS. The HPLC trace indicated the formation of three products, benzoic acid (**11a**), 2-phenyl-5-(trifluoromethyl)-1,3,4-oxadiazole (**14**), and 2,2,2-trifluoro-*N*′-(trifluoroacetyl)acetohydrazide.[6a] The peaks were compared with authentic samples by UV, MS, retention time, and co-injection.

5.12. Synthesis of 'solution phase model compound 18' (Scheme 8)

5.12.1. 2,4-Dimethoxybenzaldehyde benzoylhydrazone (16). 2,4-Dimethoxybenzaldehyde (**15**) (2 mmol, 272.3 mg), benzoylhydrazone (**2a**) (2 mmol, 332.3 mg) were stirred in CH_2Cl_2 (10 mL) containing HOAc (10 μL) for 24 h at rt. The resulting precipitation was completed upon addition of EtOEt (30 mL). The product was filtered and washed with EtOEt. Yield: 510.4 mg (89.8%).

^{1}H NMR (500 MHz, DMSO-d_6) δ 11.70 (1H, br s, NH hydrazone), 8.73 (1H, s, CH hydrazone), 7.92 (2H, d, J=7 Hz, H2, H6 phenyl), 7.82 (1H, d, J=9 Hz, H6 2,4-dimethoxyphenyl), 7.57–7.62 (1H, t, J=7 Hz, H4 benzoyl), 7.49–7.56 (2H, dd, J=7 Hz, H3, H5 benzoyl), 6.63–6.69 (2H, m, H3, H5 2,4-dimethoxyphenyl), 3.88 (3H, s, Me), 3.85 (3H, s, Me); HRMS *m/z* calcd for $C_{16}H_{16}N_2O_3$: 285.1234 $(M+H)^+$, found: 285.1230.

5.12.2. *N′*-(2,4-Dimethoxybenzyl)benzohydrazide (17). To **16** (800 mg, 2.81 mmol) dissolved in CH_2Cl_2–HOAc (4:1, v/v) was added a complex of borane and pyridine (465 mg, 5 mmol). After 2 h, the reaction mixture was diluted with CH_2Cl_2 (20 mL) and extracted with aqueous NaOH (0.5 M). The organic phase was dried over Na_2SO_4, the salts were then removed and the products evaporated to dryness. The borane adduct of **17** was removed from the crude product by chromatography on SiO_2 using CH_2Cl_2. The desired product was eluted with CH_2Cl_2–MeOH (9:1, v/v). Yield: 701 mg (86.9%).

^{1}H NMR (500 MHz, DMSO-d_6) δ 10.05 (1H, br d, J=7 Hz, NH), 7.79 (2H, d, J=7 Hz, H2, H6 benzoyl), 7.53 (1H, t, J=7 Hz, H4 benzoyl), 7.45 (2H, t, J=7 Hz, H3, H5 benzoyl), 7.21 (1H, d, J=8 Hz, H6 2,4-dimethoxybenzyl), 6.55 (1H, d, J=2 Hz, H3 2,4-dimethoxybenzyl), 6.49 (1H, dd, J=8 Hz, J'=2 Hz, H5 2,4-dimethoxybenzyl), 5.36 (1H, q, J=6 Hz, N′H), 3.89 (2H, d, J=6 Hz, CH_2 2,4-dimethoxybenzyl), 3.80 (3H, s, Me), 3.76 (3H, s, Me); HRMS *m/z* calcd for $C_{16}H_{18}N_2O_3$: 287.1390 $(M+H)^+$, found: 287.1401.

5.12.3. *N′*-Benzoyl-*N*-(2,4-dimethoxybenzyl) benzohydrazide (18). To **17** (117 mg, 0.41 mmol) dissolved in CH_2Cl_2 (5 mL) were added benzoic anhydride (**5a**) (276 mg, 1.22 mmol) and *N*-methyl imidazole (120 μL). After three days at rt the reaction mixture was extracted successively twice with 20% aqueous HOAc, then twice with satd aqueous Na_2CO_3, and with brine. The organic phase was dried over Na_2SO_4, then absorbed onto a Celite®-plug followed by chromatography on silica with EtOAc–hexane (1:1, v/v). Yield: 113.3 mg (70.7%).

^{1}H NMR (500 MHz, DMSO-d_6) δ 10.78 (1H, br s, NH), 7.55–7.56 (4H, H2, H6 benzoyl, one conformer), 7.45–7.53, 7.33–7.45 (overlapping signals of various conformers, benzoyl), 7.25 (1H, d, J=7.3 Hz, H6 2,4-dimethoxybenzyl), 6.57 (1H, d, J=2 Hz, H3 2,4-dimethoxybenzyl), 6.54 (1H, J=8 Hz, J'=2 Hz, H5 2,4-dimethoxybenzyl), 5.26, 4.33 (2H, 2d, J=14 Hz, AB-system, br, CH_2 2,4-dimethoxybenzyl), 3.76 (3H, s, Me), 3.67 (3H, s, Me); ^{13}C NMR obtained by indirect detection (gradient HSQC and gradient HMBC spectra see Supplementary data) δ 171.9, 165.8, 160.3, 158.5, 131.9, 131.8, 131.3, 129.8, 128.3, 127.6, 127.3, 127.2, 104.4, 98.3, 55.5, 55.3, 44.9. HRMS *m/z* calcd for $C_{23}H_{22}N_2O_4$: 391.1651 $(M+H)^+$, found: 391.1652.

5.13. Oxadiazole formation in solution from 18 (Scheme 9)

Compound **18** (90 mg, 0.23 mmol) was treated with TFAA–CH_2Cl_2–TFA (20:75:5, v/v/v) 10 mL for 3 h at rt. An aliquot of 100 μL was taken, evaporated to dryness, and taken up in DMSO. The white solid was filtered off and the filtrate injected into the HPLC/MS system. All major peaks were compared with authentic samples by UV, MS, retention time, and co-injection.

Acknowledgements

We thank Federico Riccardi Sirtori and Maristella Colombo for exact mass determinations.

Supplementary data

Printout of MO calculations, gradient HSQC and gradient HMBS spectra of compound **18**; HPLC traces of oxadiazole formation on solid phase and with solution phase model **18**. Supplementary data associated with this article can be found in the online version, at doi:10.1016/j.tet.2006.08.016.

References and notes

1. For instance, recent publications: (a) Hwang, J. Y.; Choi, H.-S.; Lee, D.-H.; Gong, Y.-D. *J. Comb. Chem.* **2005**, *7*, 816–819; (b) Quadrelli, P.; Scrocchi, R.; Piccanello, A.; Pierluigi, C. *J. Comb. Chem.* **2005**, *7*, 887–892; (c) Lin, X.; Cui, S.; Wang, Y. Faming Zhuanli Shenqing Gongkai Shuomingshu 2003, 10 pp; CODEN: CNXXEV CN 1445219 A 20031001 Patent written in Chinese. Application: CN 2003-116520 20030417; (d) Severinsen, R.; Kilburn, J. P.; Lau, J. F. *Tetrahedron* **2005**, *61*, 5565–5575; (e) Hennies, H.-H.; Sundermann, C.; Buschmann, H.; Sundermann, B. PCT Int. Appl. 2004, 49 pp; CODEN: PIXXD2 WO 2004024725; (f) Zou, X.-J.; Lai, L.-H.; Jin, Gui-Y.; Zhang, Z.-X. *J. Agric. Food Chem.* **2002**, *50*, 3757–3760.
2. (a) Sauer, W. H. B.; Schwarz, M. K. *J. Chem. Inf. Comput. Sci.* **2003**, *43*, 987–1003; (b) Polanski, J.; Jarzembek, Krystyna; Lysiak, V. *Acta Pol. Pharm.* **2000**, *57*, 80–81.
3. Recent syntheses of 1,3,4-oxadiazoles from 2-acyl hydrazides: (a) Kosmrli, J.; Kocevar, M.; Polanc, S. *Synlett* **1996**, 652–654; (b) Park, Y.-D.; Kim, J.-J.; Chung, H.-A.; Kweon, D.-H.; Cho, S.-D.; Lee, S.-G.; Yoon, Y.-J. *Synthesis* **2003**, 560–564; (c) Huang, W.; Hou, X.; Li, C.; He, B. *Lizi Jiaohuan Yu Xifu* **1998**, *14*, 171–174.
4. Brown, B. J.; Clemens, I. R.; Neesom, J. K. *Synlett* **2000**, 131–133.
5. (a) Kilburn, J. P.; Lau, J.; Jones, C. F. *Tetrahedron Lett.* **2001**, *43*, 2583–2586; (b) Pauvannan, K.; Hale, R.; Sedehi, D.; Chen, T. *Tetrahedron* **2001**, *57*, 9677–9682.
6. (a) Young, J. A.; Durrell, W. S.; Dresdner, R. D. *J. Am. Chem. Soc.* **1962**, *84*, 2105–2109; (b) Earlier reports on analogous solid phase Robinson–Gabriel synthesis of oxazoles: Pulici, M.; Quartieri, F.; Felder, E. R. *J. Comb. Chem.* **2005**, *7*, 463–473; (c) TFAA-mediated Bischler–Napieralski synthesis of isoquinolines: Nagubandi, S.; Fodor, G. *Heterocycles* **1981**, *15*, 165–177.
7. Liley, M. J.; Johnson, T.; Gibson, S. E. *J. Org. Chem.* **2006**, *71*, 1322–1329.
8. (a) Kikugawa, Y.; Kawase, M. *Synth. Commun.* **1979**, *9*, 49–52. The mildness of this reducing agent allows it to be used even with proteins; (b) Wong, W. S. D.; Osuga, D. T.; Feeney, R. E. *Anal. Biochem.* **1984**, *139*, 58–67; Analogous complexes have been reported to give reductions with hydrazides:

(c) Miyamura, T.; Egashira, T.; Sano, M.; Bendiak, B. K.; Kato, I. PCT Int. Appl. 2002, 42 pp; CODEN: PIXXD2 WO 2002012254 A1 20020214; Application: WO 2001-JP6524 20010730. Priority: JP 2000-234508 20000802. CAN 136:184050 AN 2002:123019; (d) Perdicchila, D.; Licandro, E.; Maiorana, S.; Baldoli, C.; Giannini, C. *Tetrahedron* **2003**, *59*, 7733–7742.

9. (a) Bouget, K.; Aubin, S.; Delcros, J.-G.; Arlot-Bonnemains, Y.; Baudy-Floc'h, M. *Bioorg. Med. Chem.* **2003**, 4881–4889; (b) Dugave, C.; Demange, L. *Lett. Pept. Sci.* **2003**, *10*, 1–9; (c) Hidaka, K.; Kimura, T.; Hayashi, Y.; McDaniel, K. F.; Dekhtyar, T.; Colletti, L.; Kiso, Y. *Bioorg. Med. Chem. Lett.* **2003**, *13*, 93–96; Guide-Jampel, E.; Chalecki, Z.; Bassir, M.; Gelo-Pujic, M. *Tetrahedron* **1996**, *52*, 4397–4402.
10. Eglington, G.; Jones, R. H.; Shaw, B. L.; Whiting, M. C. *J. Chem. Soc.* **1954**, 1860–1865.
11. Zhao, H.; Burke, T. R. *Tetrahedron* **1997**, *53*, 4219–4230.
12. Oxadiazolinium-intermediates like proposed **12a–q** have been reported earlier, for instance: Molina, P.; Tarraga, A.; Espinoas, A. *Synthesis* **1988**, 690–693.
13. A similar transacylation followed by oxadiazole formation was described by: Hassan, M. A.; Mohamad, M. M.; Shiba, S. A.; Abou-El-Regal, M. K.; Ali, A. K. *J. Saudi Chem. Soc.* **2003**, *3*, 389–396.
14. (a) Hiller, W. *Z. Kristallogr.* **1996**, *211*, 747–749; (b) Rodiou, D. C.; Kokkou, S. C.; Rentzeperis, P. J. *Acta Crystallogr., Sect. B* **1981**, *37*, 989–991; (c) Raj, S. S. S.; Yamin, B. M.; Boshaala, A. M. A.; Tarafder, M. T. H.; Crouse, K. A.; Fun, H.-K. *Acta Crystallogr., Sect. C* **2000**, *56*, 1011–1012.
15. Reynolds, C.; Hormann, R. E. *J. Am. Chem. Soc.* **1996**, *118*, 9395–9401 and references therein.
16. (a) Samdal, S.; Mollendal, H. *J. Phys. Chem. A.* **2003**, *107*, 8845–8850; (b) Chakravorty, S.; Reynolds, C. H. *J. Mol. Graphics Modell.* **1999**, *17*, 315–324.
17. Wang, Z. Y. U.S. Pat. Appl. Publ. 2003; 15 pp; CODEN: USXXCO US 2003010963 A1 20030116 CAN 138:114780 AN 2003:42708.
18. Colombo, M.; Riccardi-Sirtori, F.; Rizzo, V. *Rapid Commun. Mass Spectrom.* **2004**, *18*, 511–517.
19. Grekov, A. P.; Shvaika, O. P. *Zh. Obshch. Khim.* **1960**, *30*, 3802–3806.